Differential Cross-section Measurements for ^{3}He Elastic Scattering on ^{16}O and ^{27}Al

To cite this article: F Maragkos *et al* 2022 *J. Phys.: Conf. Ser.* **2326** 012011

View the article online for updates and enhancements.

Differential Cross-section Measurements for ^{3}He Elastic Scattering on ^{16}O and ^{27}Al

F Maragkos[1], K Bosmpotinis[1], D Cosic[2], S Fazinić[2], V Foteinou[3], M Kokkoris[1], M Krmpotić[2], N Patronis[4], G Provatas[2], E Taimpiri[1] and Th Tsakiris[1]

[1] *Department of Physics, National Technical University of Athens, Zografou Campus, 15780 Athens, Greece*

[2] *Division of Experimental Physics, Ruđer Bošković Institute, Bijenička cesta 54, 10000 Zagreb, Croatia*

[3] *Ruhr University Bochum, Central Unit for Ion Beams and Radionuclides (RUBION), Universitaetsstrasse 150, 44801 Bochum*

[4] *Department of Physics, University of Ioannina, 45110 Ioannina, Greece*

Corresponding author email: fotismaragkos@mail.ntua.gr

Abstract. In the present work measurements to determine the differential cross section values for the elastic scattering of ^{3}He on ^{16}O and ^{27}Al were carried out at the Ruđer Bošković Institute (RBI) Tandem Accelerator Facility in Zagreb, Croatia, covering the $E_{3He,lab}$=3500-5600 keV energy range, using four Silicon Surface Barrier (SSB) detectors positioned at the backscattering angles of 130º, 145º, 157.7º and 165º. The target was constructed at the facility and was comprised of a thin, self-supporting aluminum foil, upon which a thin layer of ^{nat}B (isotopic ratio: ^{11}B 80.1%, ^{10}B 19.9%), along with ^{12}C, ^{14}N, ^{16}O, was deposited using the sputtering technique. In addition, an ultra-thin layer of ^{197}Au was evaporated on top for wear protection and normalization purposes.

1. Motivation

Aluminum exhibits some remarkable properties, in particular its low weight, corrosion resistance, superb thermal and electrical conductivity and its non–toxicity, which have established it as one of the most widely used metals in the industrial and technological fields with applications ranging from the construction of automobiles, airplanes and spacecrafts, to its use in transformers, capacitors and conductors. The presence of oxygen in samples on the other hand, while not always intentional, is usually expected due to its prevalence in the Earth's atmosphere and crust. In addition, aluminum oxide is a very common catalyst in industrial processes. As a result, least destructive experimental methods that can accurately determine and quantify depth profile concentrations of these elements in near surface layers are highly desirable. Ion Beam Analysis fulfills these requirements via a combination of the Elastic Backscattering Spectroscopy (EBS) and Nuclear Reaction Analysis (NRA) techniques, mainly with a proton or deuteron beam. A beam of ^{3}He, however, offers superior mass resolution, while its use is not accompanied by the high emission of neutrons, as is the case of deuterons. Unfortunately, the use of ^{3}He beams is currently impeded by a certain lack of experimental datasets. More specifically for ^{3}He on ^{27}Al there are a only few cross section datasets, most of them at energies not suitable for IBA applications with the exception of only one dataset for the ^{27}Al(^{3}He,^{3}He$_0$)^{27}Al elastic scattering [1]. For ^{16}O more datasets are available, but again, most of them are not suitable for IBA applications. Thus the aim of this work is to determine the differential cross section values for the elastic scattering of ^{3}He on ^{16}O and ^{27}Al. These measurements, which will be made available soon to the scientific community via the IBANDL online library https://www-nds.iaea.org/exfor/ibandl.htm, are intended to play a supplementary role to measurements for NRA purposes which will be the subject of a future work.

2. Experimental Setup

The measurements were carried out at the Ruđer Bošković Institute (RBI) Tandem Accelerator Facility in Zagreb, Croatia, covering the energy range between $E_{3He,lab}$=3500-5600 keV with a 100 keV energy step. Four Silicon Surface Barrier (SSB) detectors were positioned at the 130°, 145°, 157.7° and 165° backscattering detection angles. Standard NIM electronics were utilized for data acquisition with the calibration of the ADCs being implemented using the position of the $^{197}_{79}Au\left(d,d_0\right)$ peak in the spectra.

The target used for the cross-section measurements was constructed at the facility and it consisted of 3 layers. The first layer was a thin aluminum foil acting as the backing of the target, created via evaporation. On top of it a thin layer of ^{nat}B was deposited with the use of magnetron sputtering along with ^{16}O, accompanied by ^{12}C and ^{14}N contaminants. The final layer was an ultra-thin ^{197}Au layer that was evaporated on the target surface for wear protection and normalization purposes. The evaporation took place at the Tandem Accelerator facility of NCSR "Demokritos" in Athens, Greece. The target composition was determined with complementary proton beam measurements (fig. 1) that were carried out at RBI ($E_{p,lab}$ = 1050, 1150 keV, θ = 165°) and NCSR "Demokritos" ($E_{p,lab}$ = 2750, 2920 keV, θ = 140°, 160°), using the available evaluated cross section datasets for the elastic scattering of protons on the target isotopes. In the case of ^{11}B no evaluated data exist, thus 2 different experimental datasets [2], [3] were used in an energy range (between 2700 to 3000 keV) where both of them showed good agreement. Finally, an additional measurement for the accelerator energy calibration was carried out at RBI with a proton beam at 1735 keV and a thin carbon foil using the resonance of the $^{12}C(p,p_0)$ elastic scattering at 1734 keV [4]. A -2 keV offset from the nominal beam energy was thus determined, along with an estimated ripple of ~ 6 keV (roughly equal to two channels of the ADCs).
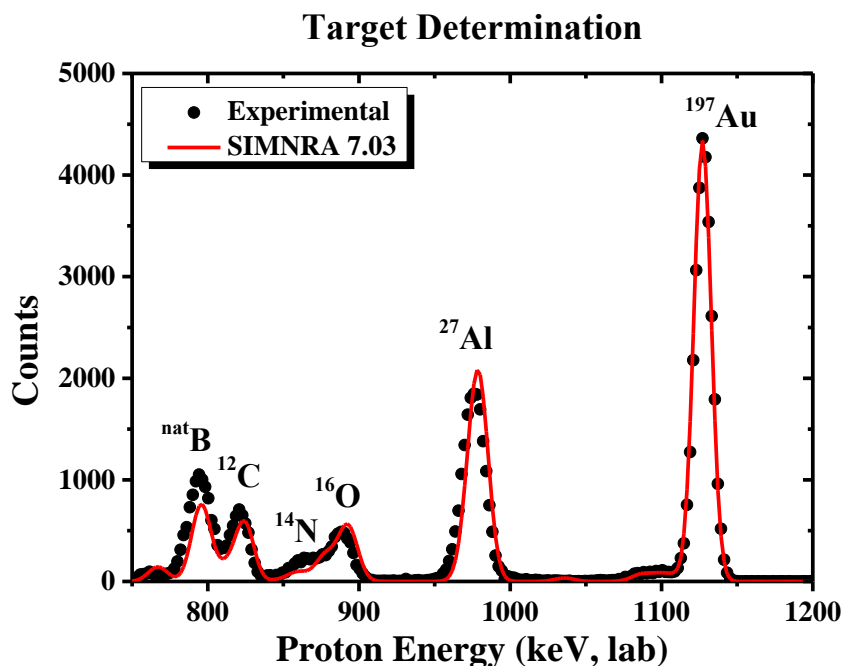

Fig. 1: Typical proton experimental and simulated spectra (black points and red line respectively) for $E_{p,lab}$ = 1150 keV and θ = 165° for the determination of the target composition.

3. Data Analysis

To determine the differential cross section values the relative measurement technique was used:

$$\left(\frac{d\sigma}{d\Omega}\right)_{isotope}^{E,\theta} = \left(\frac{d\sigma}{d\Omega}\right)_{^{197}Au}^{E',\theta} \frac{N_{^{197}Au}}{N_{isotope}} \frac{Y_{isotope}}{Y_{^{197}Au}} \tag{1}$$

where θ represents the detection angle, E the energy in the middle of the target thickness and E′ the beam energy reaching the target surface, having taken into account the accelerator energy calibration in both cases. The term $\left(\frac{d\sigma}{d\Omega}\right)_{Au}^{E',\theta}$ represents the screened Rutherford cross section values of the ^{197}Au-^{3}He elastic scattering according to L' Ecuyer et al. [5]. The terms $N_{^{197}Au}$ and $N_{isotope}$ refer to the atomic areal densities of the ^{197}Au layer and the isotope under investigation respectively. To determine these values, the SIMNRA code version 7.03 [6] was used along with the aforementioned proton experimental spectra at $E_{p,lab}$ = 1050, 1150, 2750 and 2920 keV. For ^{16}O and ^{27}Al, evaluated cross sections were used provided by the SigmaCalc 2.0 online calculator, http://sigmacalc.iate.obninsk.ru/, whereas for ^{197}Au the values were calculated via the Rutherford formula. In each case the proton energies were selected so as to exclude any significant cross section variations due to the existence of Breit–Wigner type resonances and, for ^{16}O specifically, to avoid possible overlapping peaks in the spectra. The average value determined for ^{16}O was (372.9 ± 17.1)×10^{15} atoms/cm^2, for ^{27}Al (649.3 ± 5.1)×10^{15} atoms/cm^2 and for ^{197}Au (31.8 ± 5.6)×10^{15} atoms/cm^2 utilizing the ZBL stopping power compilation [7].

Finally, the terms $Y_{isotope}$ and $Y_{^{197}Au}$ refer to the integrated yield of the corresponding elastic peak in the experimental spectra (fig. 2), analyzed using the SPECTRW [8] code. The spectra were quite complex, mainly due to the presence of reaction peaks overlapping with the elastic peaks, especially for higher energies and lower detection angles, along with the low current of the beam during the measurements. Moreover, ^{12}C and ^{16}O produced multiple peaks because they were present in all the layers of the target. In addition, for a number of these reactions there are no available cross section data. As a consequence, reliable, high-accuracy results could be obtained only for certain energies for the elastic scattering of ^{3}He particles on ^{16}O and ^{27}Al and for 3 backscattering detection angles, namely at 145°, 157.7° and 165°.

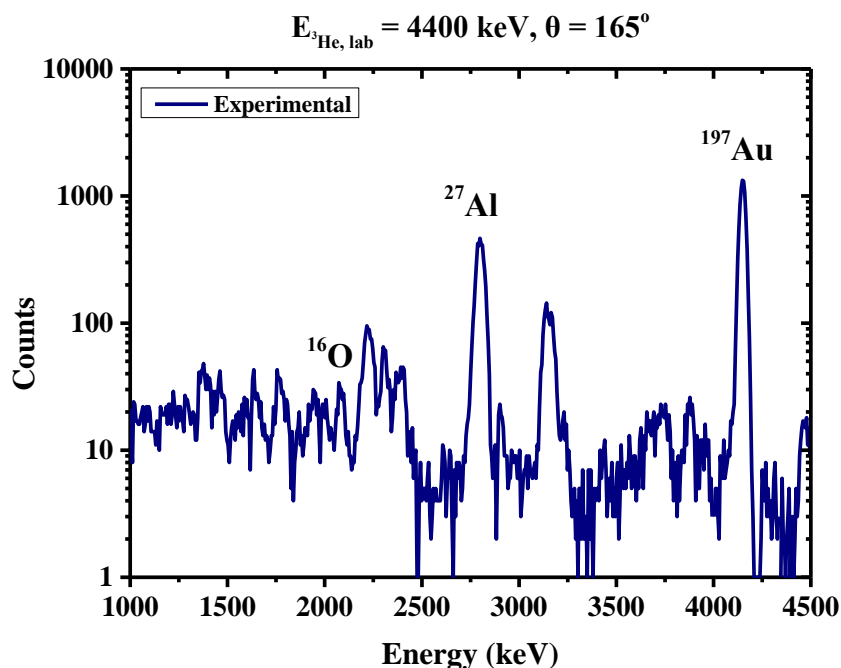**Fig. 2**. A typical experimental ^{3}He spectrum for $E_{3He,lab}$ = 4400 keV, θ = 165°

4. Results and Conclusions

The differential cross section values for the elastic scattering of ^{3}He on ^{16}O and ^{27}Al as determined by formula 1, are shown in figs. 3a-c and 4a-c respectively (black points) along with the available data from literature (blue points) and the Rutherford values (red line). In the case of ^{16}O, the acquired data correspond to the beam energy in the middle of the target, taking into account the accelerator calibration and the energy loss of the beam determined using the SIMNRA code. The total relative statistical uncertainty was around 10%, however, the uncertainties of the last four data points were between 17 to 23% due to the low statistics in the experimental spectra. The data exhibit strong deviations from the Rutherford values (red line), which could be attributed to overlapping resonances from the energy levels of the compound nucleus ^{19}Ne* [9]. The only available comparable dataset in literature was measured by Ropke et al. [10] (blue points) showing a reasonably good agreement with the acquired data in the present work, for the few energies where the two datasets overlapped.
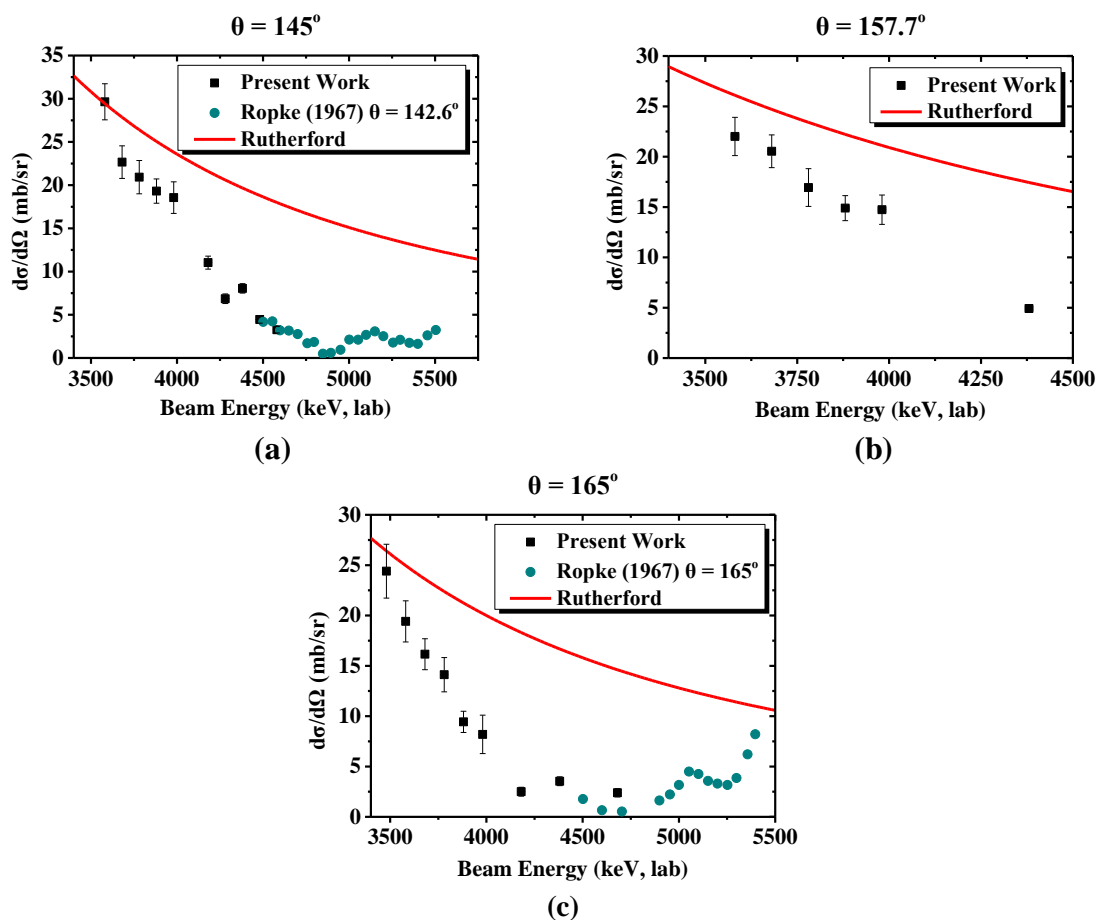

Fig. 3a-c: Comparison between the acquired differential cross section values (mb/sr) of the elastic ^{16}O(^{3}He,^{3}He$_0$)^{16}O scattering (black points), the corresponding Rutherford values (red line) and the values by Ropke et al. (blue points) for the scattering angles of 145° (a), 157.7° (b), 165°(c)

In the case of ^{27}Al, the obtained differential cross-section values correspond to the beam energy at the middle of the aluminum layer of the target, again after first taking into account the accelerator energy calibration and the beam energy loss. The total relative statistical uncertainty did not exceed 6%. No pronounced structure can be seen in the cross sections (black points) and there is no available information about the structure of the compound nucleus ^{30}P* in this energy range [11]. In addition, deviations from the corresponding Rutherford values (red line) are observed at higher energies, becoming progressively more prominent. Again, there is only one available dataset for the elastic

scattering of ^{3}He on ^{27}Al, at energies comparable to the present work, by C.S. Lin et al. [1] (blue points). The trend of the datasets appears to be in very good agreement with the points for the common energies exhibiting only small discrepancies.

Finally, it should be noted that in both cases only the total statistical uncertainties are plotted and no systematic uncertainties are included in figs 3 and 4. The systematic uncertainties originate mainly from the accuracy of the implemented stopping power models and from possible lateral inhomogeneities of the target. The differential cross-section datasets obtained in the present work constitute a coherent set, suitable for selected EBS applications. When similar NRA datasets also become available, the joint implementation of the EBS and NRA techniques is expected to yield high-accuracy results concerning the determination of depth profile concentrations of oxygen and aluminum in a large variety of matrices.
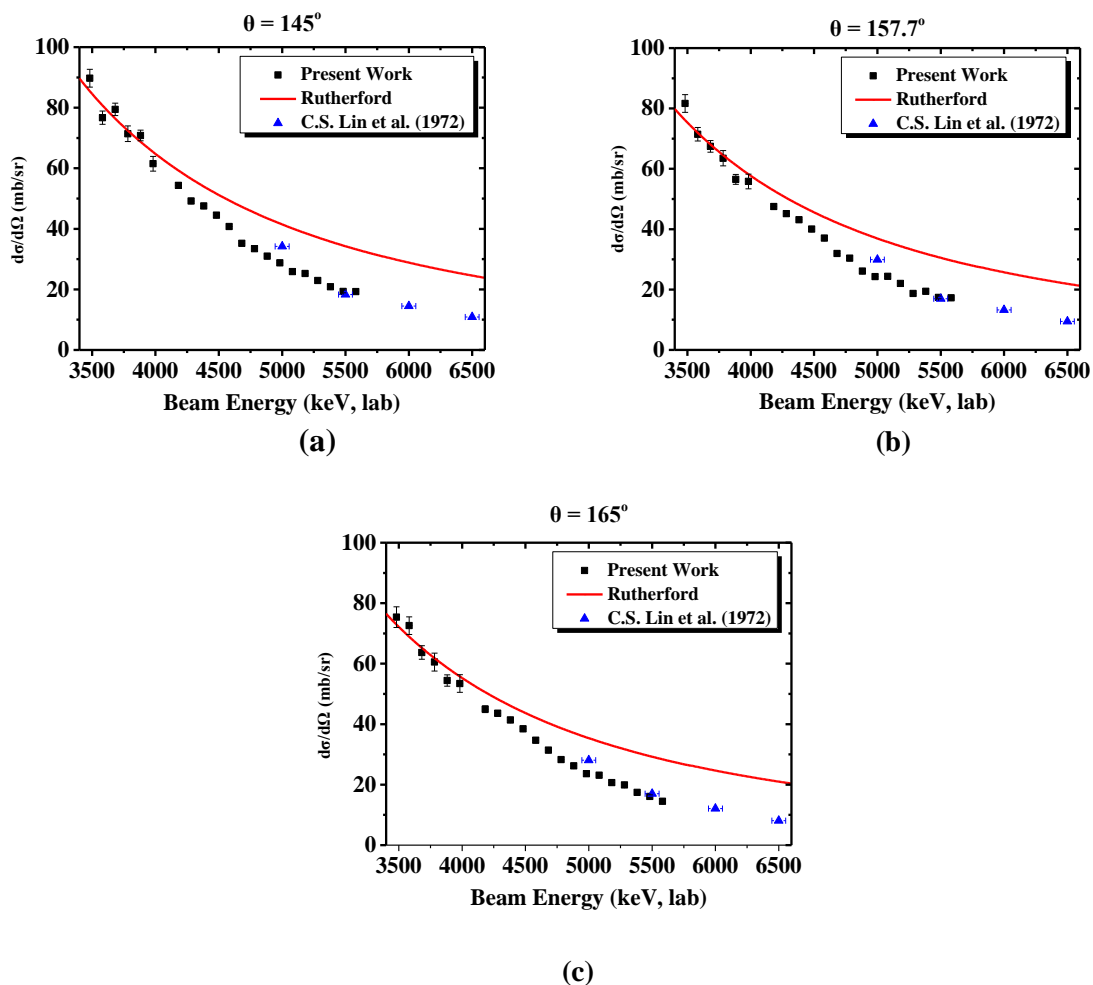

Fig. 4a-c: Comparison between the acquired differential cross section values (mb/sr) of the elastic ^{27}Al(^{3}He,^{3}He$_0$)^{27}Al scattering (black points), the corresponding Rutherford values (red line) keV and the data by C.S. Lin et al. (blue points) for the scattering angles of 145° (a), 157.7° (b), 165° (c)

References

[1]   Lin C S, Lin E K, Song P S, Wen-Ming, Meng H C, Wung C C, Chou J C Chinese Journal of Physics (Taiwan), Vol.10, p.84
[2]   Kokkoris M, Kafkarkou A, Paneta V R, Misaelides P and Lagoyannis A 2010 *Nucl. Instr. Meth. B* **268**, p.3539-3545
[3]   Chiari M, Giuntini L, Mandò P A and Taccetti N 2001, *Nucl. Instr. Meth. B* **184**, p. 309-318
[4]   Santra S, Mahata K, Singh P, Fernandes C V, Hemalatha M, Kailas S 2003 *Nucl. Instr. Meth. A 496, p. 44-50*
[5]   L'Ecuyer J, Davies J A and Matsunami N 1979, *Nucl. Instr. Meth* **160**, p. 337-346
[6]   Mayer M 2014, *Nucl. Instr. Meth. B* **332**, p. 176-180
[7]   Ziegler J F, Biersack J P, Littmark U, Anderson H H *1985, Pergamon Press, New York*
[8]   Kalfas C A, Axiotis M and Tsabaris C 2016, *Nucl. Instr. Meth. A* **830**, p. 265-274
[9]   Tilley D R, Weller H R, Cheves C M, Chasteler R M 1995 *Nucl. Physics A* **595**, p. 1-170
[10]   Ropke H, Lieb K P and Konig R 1967 *Nucl. Physics A* **97**, p. 609-619
[11]   Shamsuzzoha Basunia M 2010 *Nucl. Data Sheets* **111**, p. 2331-2424